Theoretical Modeling and Simulation of Airflow Field near Grinding Wheel

Z. L. Han and C. H. Li*

School of Mechanical Engineering,
Qingdao Technological University, 266033 China

**Corresponding Author: Li C.H. E-mail: sy_lichanghe@163.com*

Abstract

During the grinding, the principal axis drives the grinding wheel to rotate at a high speed, which generates disturbance to the air flows around the grinding wheel. Therefore, a layer of air boundary can be formed on the surface of the working grinding wheel, which is the airflow field. Airflow field not only affects the machining accuracy of the workpiece and the enhanced abrasion of grinding wheel, but also prevents the efficient injection of the grinding fluid into the grinding zone. These processing conditions and lead to the increasing grinding force and rising grinding temperature, deteriorating the processing quality and surface integrity of the workpiece. With higher rotation speed of grinding wheel, the "airbond" of the air flow will be greater. And the grinding fluid will be harder to break through the "airbond" and be supplied to the grinding zone. In this study, on the basis of theoretical analysis on the airflow field of grinding wheel, a mathematical model was established, including the internal and external pressure differences of the airflow field, the airbond thickness δ, fluid density ρ, radius R and radius ω. In addition, the changing rules of airflow field along the grinding wheel were studied based on simulation tests. Results demonstrate that the tested airflow field presented the same pressure in concentric circles of the grinding wheel. Along the surface outer normal direction, the pressure value gradually decreased from the outer to the inner space, presenting negative pressure gradient. The velocity of the airflow field around the grinding wheel reduced as the distance from the wheel increased. To a certain thickness, the velocity became zero, which verified the existence of the boundary layer.

Keywords: *Grinding wheel; Airflow field; Airbond; Pressure; Velocity*

1. Introduction

Grinding, as the most important approach for precision machining, has been gaining more attentions from people. The most important feature of grinding is the high rotation speed of grinding wheel driven by the principal axis. Therefore, at the condition of high-speed revolution, a boundary layer formed on the grinding wheel, which is the airflow field. Airflow field around the grinding wheel is inevitable in the grinding and machining. The velocity, pressure and distribution patterns of airflow field in the grinding zone are crucial in various aspects, including machining precision and surface integrity of components, the abrasion of grinding wheel and the effective injection of the grinding fluid into the grinding zone. As a result, correct knowledge of the velocity and the pressure distribution rules of grinding wheel field in the grinding zone are of great significance to the further control and application of the airflow field in the industrial production.

As a boundary layer exists around the grinding wheel, the grinding fluid is prevented from easily entering the grinding zone. S. Ebbrell [1] and others conducted the modeling and tests,

exploring into the impact of the boundary layer on the effective injection of the grinding fluid into the grinding zone as well as the application of the airflow field to increase the grinding fluid flow. With the setting of three different nozzle positions, the flow of the grinding fluid passing through the grinding zone was calculated, as well as the surface roughness and dimension distribution of the workpiece. Based on experiments, it can be found that when the nozzle was located above airflow velocity of the reversed flow of the grinding zone, the flow of the grinding fluid passing through the grinding zone can be increased and the surface quality as well as dimension precision of the workpiece can be improved. Guo and Malkin [2-3] established the theoretical model of the grinding fluid passing through the grinding zone, that is, the useful flow rate. Engineer analyzed the influential factors on the useful flow rate through experiments. Y. Saito [4] and others studied on the impact of the wheel porosity on the airflow field velocity around the grinding wheel and the pressure on the grinding zone, finding that the larger the porosity, the higher the velocity and pressure in the airflow field, and the thicker the air boundary layer; J. Shibata [5] and others researched on the application of the velocity changes of the airflow field around the grinding wheel in the evaluation of grinding wheel abrasion, so as to lay a solid basis of online monitoring of the surface topography of the grinding wheel; Rahman [6] and V. Radhakrishnan [7] identified the surface roughness changes under the changing pressure in the airflow field of the grinding wheel so as to determine whether the grinding wheel should be modified for the performance of the grinding wheel. In this paper, the author applied ANSYS to simulate the airflow field in the grinding zone on the computer. The airflow field was simulated and analyzed at different rotational speeds of the grinding wheel and with different clearance between the grinding wheel and the workpiece. The results showed that with the elevated velocity of the grinding wheel, pressures in the airflow field of the grinding zone were increased accordingly.

2. Surface Airbond Analysis

There are generally four revolution airflows on the highly-rotated grinding wheel, including the circumferential circulation, saturated flow, internal flow and radial flow. This is caused by the friction between the wheel surface and the air as well as the centrifugal force. As the CBN grinding wheel with the metal substrate does not have pores, it does not present saturated flow and internal flow but the circumferential circulation and radial flow, as shown in Figure 1. Circumferential circulation refers to the airflow circumferentially rotating around the grinding wheel, which impedes the supply of the grinding fluid. Radial flow is formed by the interactions between the wheel surface and the air as well as the centrifugal force, which does not influence much on the supply of the refrigerant.

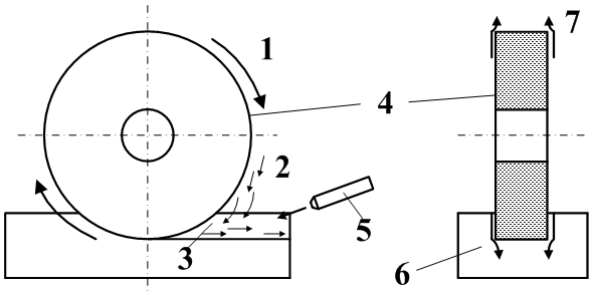

Figure 1. Surface Airbond Analysis

1. Circumferential circulation; 2. Refrigerant; 3. Airbond; 4. Grinding Wheel; 5. Nozzle; 6. Workpiece; 7. Radial Flow

Gases have elasticity and fluidity. To exert pressure on the gas, the volume of gas will be changed. The elasticity of gases is defined as the incremental ratio between the pressure increments and the unit specific volume of gas. Specific volume is the volume occupied by the unit mass, which is equal to the reciprocal of the density. Unit specific volume increment is $d[1/\rho]/(1/\rho) = d\rho/\rho$. The modulus of elasticity is defined as [8-11]:

$$E = -\frac{dp}{d(1/\rho)/(1/\rho)} = \rho\frac{dp}{d\rho} \tag{1}$$

Where $d\rho/\rho$ is equal to squared sonic velocity. All fluids have fluidity, which is the relative air fluidity in aerodynamics. As the grinding wheel rotates in the air, air in the vicinity of its movement area will be pushed away by the grinding wheel so that the grinding wheel can get through. The pushing fluid motion is regarded as the disturbed movement. In fact, the disturbed movement does not just involve those air micelles that directly contact with the grinding wheel because fluids have fluidity [12-15]. The disturbed movement spreads the disturbance from the near to the distant through the interactions between the micelles. The layer-by-layer spreading of disturbance is related with the viscosity of the air. In accordance with the above equation, it is related with sonic velocity. If the disturbance is not very strong, this spreading velocity is equal to the sonic velocity.

Given that the speed of the fluid in direct contact with an object must be zero (assume the object does not move) and a great flow velocity exists from the object surface, if the flow rate changes as such in a short distance along the normal direction of the object plane, the normal gradient of the velocity must be very large, since the viscosity force cannot be ignored. The layer of fluid that closely attaches to the object plane under the role of the viscosity force is called as the boundary layer. The larger the Reynolds number of the entire flow field is, the thinner this layer will be [16]. Thus, at the premise of a large Reynolds number, the flow field is divided into two parts: one in the boundary layer, which needs to consider the inertial force and the viscous force; the other one is the massive flow field out of the boundary layer, where the flow is potential flow. As the boundary layer is very thin under a large Reynolds number, the boundary layer cannot impose a great impact on the entire potential flow field.

3. Theoretical Modeling of the Airflow Field of Grinding Wheel

At a place near the grinding wheel surface, a rectangle air flow infinitesimal was selected, and the gravity of infinitesimal was ignored. Set the external normal direction of the grinding wheel as Y-axis direction and the tangential direction as the X-axis direction, and the air infinitesimal stress is shown in Figure 2. According to the principles of Newtonian mechanics, the air infinitesimal stress meets Eq. (2):

$$\begin{cases} F_x = \tau_1 A - \tau_2 A = 0 \\ F_y = dF - dpdA = 0 \end{cases} \tag{2}$$

Where $\tau_1 A$—friction of grinding wheel surface to the air infinitesimal; $\tau_2 A$—friction of upper fluid to the air infinitesimal; *dF*—the centrifugal force on the air infinitesimal in an equilibrium state; *dpdA*—surface force due to the air pressure difference on the surface of the grinding wheel.

And we can obtain that:

$$dp = \frac{dF}{dA} \tag{3}$$

According to Eq. (3), the pressure difference on the upper and lower surfaces of the air infinitesimal was generated by the centrifugal force, *i.e.*, the centrifugal force causes surface pressure gradient of the grinding wheel. The centrifugal force equation of rotational movement can be expressed as:

$$F = mR\omega^2 = \rho VR\omega^2 \tag{4}$$

To substitute the above equation into Eq. (3) and we obtain:

$$dp = \frac{\rho R\omega^2 dV}{dA} = \rho R\omega^2 dy \tag{5}$$

Where *R*—radius of grinding wheel; dy— height of the air infinitesimal.

According to the boundary layer theory of Ludwig Prandtl, when the grinding wheel rotates, only a thin layer of air, which closes to the grinding wheel, will be greatly influenced by the viscosity force, and the viscosity force from the external fluid only imposes insignificant impact on the fluid motion. Hence, this layer is known as the airbond. Thus, for the flow field on the wheel surface in this model, the fluid motion is only intense in the airbond, and the fluid out of the airbond almost remained the original state of rest. Therefore, the air infinitesimal stress in the airbond should be calculated. No plastic flow was tested out of the boundary layer and the grinding wheel rotation does not influence over the flow field pressure. According to the hydromechanics, the fluid only has the X-axis velocity and zero Y-axis velocity. X-axis velocity was inversely proportional to the radius $u_x = \frac{C}{R}$. At the equilibrium state, the linear state of the empty airflow field is shown in Figure 3.

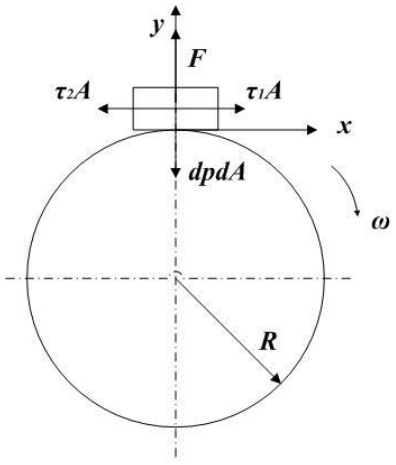

Figure 2. Physical Model

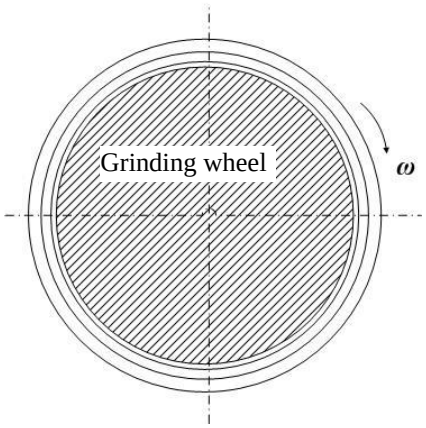

Figure 3. Linear Figure of the Air Flow around the Grinding Wheel

To specify the fluid motion of an object, the Navier – Stokes Equation (referred to as N-S Equation), should be established. According to two-dimensional N-S equation, the following steady flow equation set was established, with the consideration of the centrifugal force [16-18]:

$$\begin{cases} u_x \dfrac{\partial u_x}{\partial x} + u_y \dfrac{\partial u_x}{\partial y} = -\dfrac{1}{\rho}\dfrac{\partial p}{\partial x} + \nu\left(\dfrac{\partial^2 u_x}{\partial x^2} + \dfrac{\partial^2 u_x}{\partial y^2}\right) \\ u_x \dfrac{\partial u_y}{\partial x} + u_y \dfrac{\partial u_x}{\partial y} = -\dfrac{1}{\rho}\dfrac{\partial p}{\partial y} + \nu\left(\dfrac{\partial^2 u_y}{\partial x^2} + \dfrac{\partial^2 u_y}{\partial y^2}\right) + \dfrac{u_x^2}{R} \\ \dfrac{\partial u_x}{\partial x} + \dfrac{\partial u_y}{\partial y} = 0 \end{cases} \tag{6}$$

With the comparison of the order of magnitudes in the equation, the small amount was divided out and the final form of the equation is as follows[19]:

$$\begin{cases} u_y \dfrac{\partial u_x}{\partial y} = \nu \dfrac{\partial^2 u_x}{\partial y^2} \\ \dfrac{1}{\rho}\dfrac{\partial p}{\partial x} = 0 \\ \dfrac{1}{\rho}\dfrac{\partial p}{\partial y} = \dfrac{u_x^2}{R} \end{cases} \tag{7}$$

It can be seen that: X-axis pressure gradient is 0, and Y-axis pressure gradient is $\dfrac{dp}{dy} = \rho\dfrac{u_x^2}{R}$. As u_x is linearly distributed in the airbond, we set the airbond thickness as δ. According to the boundary conditions, we obtain [20]:

$$\begin{cases} u_x = R\omega; \ \ y = 0 \\ u_x = 0; \ \ y = \delta \end{cases} \tag{8}$$

The X-axis velocity in the airbond is:

$$u_x = R\omega\left(1 - \frac{y}{\delta}\right) \tag{9}$$

To substitute Eq. (9) into the Y-axis pressure gradient equation, we obtain [21-22]:

$$\frac{dp}{dy} = \rho\frac{1}{R}R^2\omega^2\left(1 - \frac{y}{\delta}\right)^2 = \rho R\omega^2\left(1 - \frac{y}{\delta}\right)^2 \tag{10}$$

With the integral of the above equation in the airbond, the internal and external pressure difference of the airbond is:

$$\Delta p = \int_0^\delta \rho R\omega^2\left(1 - \frac{y}{\delta}\right)^2 dy = \frac{1}{3}\delta\rho R\omega^2 \tag{11}$$

If Eq. (9) is transformed into the angular velocity of the rotating fluid within the airbond, we obtain:

$$\omega' = \frac{u_x}{R} = \omega\left(1 - \frac{y}{\delta}\right) \tag{12}$$

To substitute the above equation into Eq. (5), we obtain [23-24]:

$$dp = \rho R\omega^2\left(1 - \frac{y}{\delta}\right)^2 dy \tag{13}$$

It can be seen from Eq. (11) that the factors affect the pressure difference inside and outside of the airbond include the airbond thickness δ, the fluid densityρ, the radius of the grinding wheel R and the rotation angular velocity of the grinding wheel ω. Δ is highly related with the fluid viscosity. The larger the viscosity, the thicker the boundary thickness will be, and vice versa.

Under standard atmospheric pressure, the air density at a room temperature of 20℃, ρ=1.225kg/m^3, the rotational angular velocity of the grinding wheel is ω=450r/s. Assume δ is 1mm. To substitute the value in Eq. (11), we obtain:

$$\Delta p = \frac{1}{3}\delta\rho R\omega^2 = \frac{1}{3}\times 1\times 10^{-3}\times 1.225\times 100\times 10^{-3}\times 450^2 = 8.26Pa \tag{14}$$

As the density and viscosity of the air is relatively small, it can be calculated that the internal and external pressure difference of the airbond is relatively small. The empty airflow field in the airbond along the external normal direction of the wheel surface presented negative pressure gradient, which can be calculated from Eq. (10). Meanwhile, the air flow out of the airbond showed no viscous flow and unchanging pressure.

Therefore, with relatively small density and viscosity of the air as well as relatively small internal and external pressure difference of the airbond, the airbond thickness is very small [25-28]. Yet, the internal fluid motion is very complex and intense. In the airbond, the negative pressure gradient attaches the air on the wheel surface. If the negative pressure gradient is used on the grinding fluid, it can promote the grinding fluid to enter the wedge-clearance between the grinding wheel and the workpiece.

4. Simulation of the Airflow Field of Grinding Wheel

When the grinding wheel rotated in the air, the axial length does not affect the empty airflow field distribution around the grinding wheel. Thus, a two-dimensional model was created in the simulation. Simulation parameters were shown in Table 1. 2D single precision solver in FLUENT was used to calculate. The boundary conditions were set as the pressure-outlet and the rotational angular velocity of the grinding wheel was set as 450r/s.

Table 1. Simulation Parameters of Wheel Flow Field

Items	Values
Diameter (mm)	200
Width (mm)	30
Outer Boundary Diameter (mm)	600
Angular Velocity of Grinding Wheel (r/s)	450

The boundary conditions were initialized and appropriate convergence conditions were set. With a certain number of iteration steps, the final calculation results were obtained. Figure 4 shows the pressure contour cloud diagram of the circumferential flow of the grinding wheel. Figure 5 shows the enlarged drawing of the pressure contour on the wheel surface.

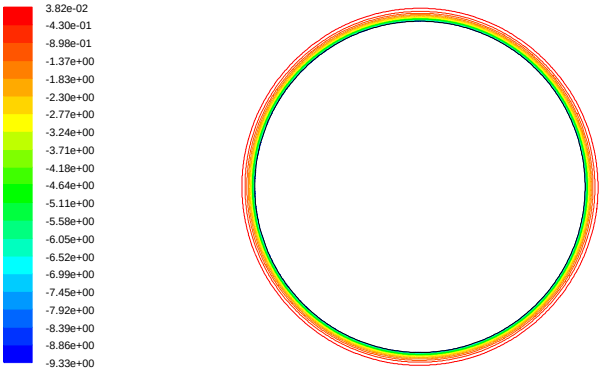

Figure 4. Cloud Drawing of Pressure Contour around the Grinding Wheel

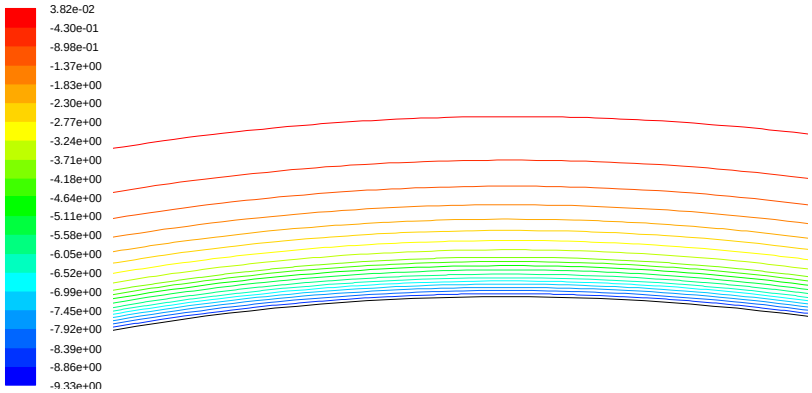

Figure 5. Enlarged Drawing of the Pressure Contour on the Wheel Surface

It can be seen from Figure 4 that the static pressure in most areas of the computational domain was close to 0 (the operating pressure was 101325 Pa. Unless stated, all pressure values in this paper were values of relative pressure). Only a thin layer of fluid close to the wheel surface presented negative pressure. In Figure 5, it can be observed that pressure contours were concentric circles, and the air pressure of the layer closest to the wheel surface was -9.33Pa; from the internal to external layer, the pressure gradually increased. The pressure of the outermost external was 0.03Pa, showing the tendency of gradual increase. In the boundary layer, the innermost air pressure was deducted by the outermost air pressure, reaching the pressure differential of 9.36Pa, which was basically consistent with the theoretical results of Equ. 13. As the negative surface pressure of the grinding wheel was lower than the external pressure, which was thus referred to as the negative pressure area of the grinding wheel. It can also be observed from the concept of pressure gradient, the pressure gradually decreased along the exxternal normal direction of the wheel surface from the internal to external layer, and the pressure gradient was negative. This was called as the negative pressure gradient area of the grinding wheel. Thus, a boundary layer exists around the rotating grinding wheel, and the air velocity in this layer decreased as the distance from

the grinding wheel increased. To a certain thickness, the velocity was zero. The thickness can be obtained through the observation of the static pressure change curve on the direction of outer normal curve of the grinding wheel in Figure 6 as well as the velocity change curve on the direction of outer normal curve of the grinding wheel in Figure 7.

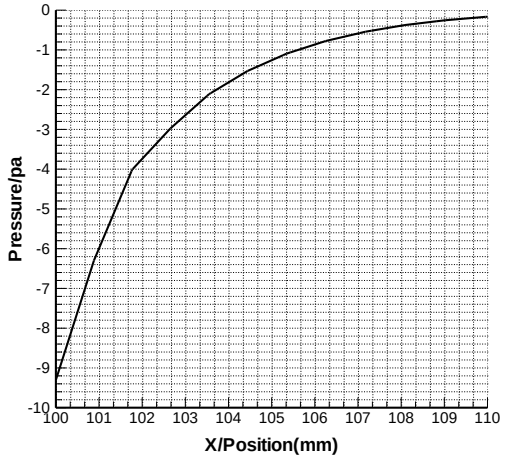

Figure 6. The Pressure Change Curve along the Normal Direction of the Grinding Wheel

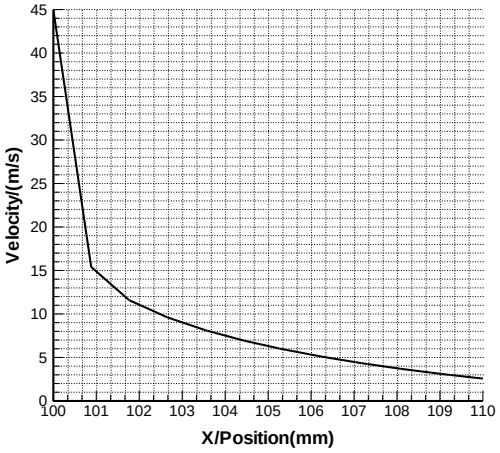

Figure 7. Velocity Change Curve along Outer Normal Direction of the Grinding Wheel

In the Figure 7, at X = 100 mm (which was closest to the wheel surface on the outer normal direction), the pressure value was -9.33pa, and the velocity was 45m/s; as X increased, the pressure value increased rapidly (the absolute value dropped). To X=101.3mm, the pressure value and the velocity change gradient were maximum, respectively as ΔP=4.30Pa and ΔV=33m/s. therefore, it can be obtained that with the simulation conditions in this paper, the thickness of the airbond around the grinding wheel δ was about 101.3-100=1.3mm, basically consistent with the results of the above theoretical calculation.

5. Impact of the Rotating Velocity of Grinding Wheel on Airbond Thickness

The diameter of the grinding wheel was 200mm and its width was 30 mm. With the above parameters unchanged, the radical pressure change can be obtained with the changes of the circumferential velocity of the grinding wheel. The circumferential velocity of the grinding wheel was taken as 45m/s, 80m/s, 120m/s and 160m/s respectively. The change curve was shown in Figure 8.

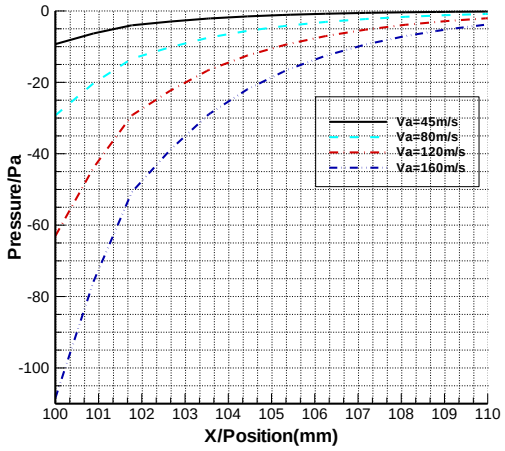

Figure 8. Pressure Change on the Outer Normal Direction with the Rotational Velocity Change

As can be seen from Figure 8, the higher the velocity of the grinding wheel was, the thicker the airbond was. A remarkable steep velocity gradient appeared on the surface of the grinding wheel. The thickness of the airbond increased as the rotation velocity of the grinding wheel increased. Specific values can be drawn according to the above method. Under the simulation conditions, when the velocity of the grinding wheel was 45m/s, δ was about 1.3mm; when the velocity was 80m/s, δ was about 1.8mm; when the velocity was 120m/s, δ was about 2.4mm; when the velocity was 160m/s, δ was about 3mm.

6.Conclusion

On the basis of the analysis results, the following conclusions are drawn:

(1) A mathematical model was established, including the internal and external pressure differences of the airflow field, the airbond thickness δ, fluid density ρ, radius R and radius ω. In addition, the changing rules of airflow field along the grinding wheel were studied based on simulation tests. Results demonstrate that the tested airflow field presented the same pressure in concentric circles of the grinding wheel. Along the surface outer normal direction, the pressure value gradually decreased from the outer to the inner space, presenting negative pressure gradient. The velocity of the airflow field around the grinding wheel reduced as the distance from the wheel increased. To a certain thickness, the velocity became zero, which verified the existence of the boundary layer.

(2) A remarkable steep velocity gradient appeared on the surface of the grinding wheel. The thickness of the airbond increased as the rotation velocity of the grinding wheel increased. Under the simulation conditions, when the velocity of the grinding wheel was

45m/s, δ was about 1.3mm; when the velocity was 80m/s, δ was about 1.8mm; when the velocity was 120m/s, δ was about 2.4mm; when the velocity was 160m/s, δ was about 3mm.

Acknowledgements

This research was financially supported by the National Natural Science Foundation of China (50875138; 51175276); the Shandong Provincial Natural Science Foundation of China (ZR2009FZ007) ; Qingdao science and technology program of basic research projects (12-1-4-4-(1)-jch).

References

[1] S. Ebbrell, N. H. Woolley, Y. D. Tridimas, D. R. Allanson and W. B. Rowe, "The effects of cutting fluid application methods on the grinding process", International Journal of Machine Tools & Manufacture, vol. 40, no. 2, **(2000)**, pp. 209–223.
[2] C. Guo and S. Malkin, "Analysis of fluid flow through the grinding zone", Journal of Engineering for Industry, vol. 114, no. 4, **(1992)**, pp. 427-434.
[3] C. Guo and S. Malkin, "Experimental measurement of fluid flow through the grinding zone", Journal of Engineering for Industry, vol. 114, no. 1, **(1992)**, pp. 61-66.
[4] Y. Saito, N. Nishiwaki and Y. Ito, "An Investigation of Local Heat Transfer During Grinding Process--Effects of Porosity of Grinding Wheel", American Society of Mechanical Engineers, vol. 101, no. 5, **(1978)**, pp. 97-103.
[5] J. Shibata, T. Goto, M. Yamamoto, *et al.*, "Characteristics of air flow around a grinding wheel and their availability for assessing the wheel wear", CIRP Annals-Manufacturing Technology, vol. 31, no. 1, **(1982)**, pp. 233-238.
[6] J. F. Rahman and V. Radhakrishnan, "Surface condition monitoring of grinding wheels by pneumatic back-pressure measurement", Wear, vol. 70, no. 2, **(1981)**, pp. 219-226.
[7] V. Radhakrishnan, J. F. Rahman, "Functional assessment of the grinding wheel surface characteristics by turbulence amplifier", J. Eng. Ind., vol. 103, no. 1, **(1981)**, pp. 99-102.
[8] M. N. Morgan, A. R. Jackson and H. Wu, "Optimisation of fluid application in grinding", CIRP Annals-Manufacturing Technology, vol. 57, no. 1, **(2008)**, pp. 363-366.
[9] N. Patir and H. S. Cheng, "An Average Flow Model for Determining Effects of Three-Dimensional Roughness on Partial Hydrodynamic Lubrication", ASME J. Lubr. Technol., vol. 100, **(1978)**, pp. 12–17.
[10] C. H. Li, Y. L. Hou, Z. Fang, *et al.*, "Analytical and experimental investigation of grinding fluid hydrodynamic pressure at wedge-shaped zone", International Journal of Abrasive Technology, vol. 4, no. 2, **(2011)**, pp. 140-155.
[11] E. Brinksmeier and E. Minke, "High-performance surface grinding— the influence of coolant on the coolant process", Annals of the CIRP, vol. 42, no. 1, **(1993)**, pp. 367–370.
[12] C. C. Chang, "An application of lubrication theory to predict useful flow-rate of coolant on grinding porous media", Tribology international, vol. 30, no. 8, **(1997)**, pp. 575-581.
[13] C. Frank, Z. Wojciech and F. Edwin, "Fluid Performance Study for Groove Grinding a Nickel-Based Superalloy Using Electroplated Cubic Boron Nitride (CBN) Grinding Wheels", Journal of Manufacturing Science and Engineering, vol. 126, no. 3, **(2004)**, pp. 451-458.
[14] F. Katsushi, O. Noriyuki, H. N. Trong and T. Nakamura. "In-process measurement of topography change of grinding wheel by using hydrodynamic pressure", International Journal of Machine Tools & Manufacture, vol. 42, no. 13, **(2002)**, pp. 1447–1453.
[15] Y. L. Hou, C. H. Li and Q. Zhang, "Investigation of structural parameters of high speed grinder spindle system on dynamic performance", Int. J. Materials and Product Technology, vol. 44, nos. 1/2, **(2012)**, pp. 92-114.
[16] C. H. Li, Y. L. Hou, Y. C. Ding and G. Q. Cai, "Feasibility investigations on compound process: a novel fabrication method for finishing with grinding wheel as restraint", International Journal of Computational Materials Science and Surface Engineering, vol. 4, no. 1, **(2011)**, pp. 55 - 68.
[17] V. K. Gviniashvili, N. H. Woolley and W. B. Rowe, "Useful coolant flowrate in grinding", International Journal of Machine Tools & Manufacture, vol. 44, no. 6, **(2004)**, pp. 629-636.
[18] C. H. Li, Y. L. Hou, Z. R. Liu and Y. C. Ding, "Investigation into temperature field of nano-zirconia ceramics precision grinding", International Journal of Abrasive Technology, vol. 4, no. 1, **(2011)**, pp. 77-89.
[19] V. Gviniashvili, J. Webster and B. Rowe, "Fluid Flow and Pressure in the Grinding Wheel-Workpiece Interface", Transactions of the ASME, vol. 127, no. 1, **(2005)**, pp. 198-205.

[20] P. Hryniewicz, A. Z. Szeri and S. Jahanmir, "Application of Lubrication Theory to Fluid Flow in Grinding: Part I-Flow Between Smooth Surfaces", Journal of Tribology ASME, vol. 123, no. 1, **(2001)**, pp. 94–100.
[21] Y. Hou, C. Li, Z. Han, **et al.**, "Examination of the Material Removal Mechanisms During the Abrasive Jet Finishing of 45 Steel", Adv. Sci. Lett., vol. 4, nos. 4-5, **(2011)**, pp. 1478-1484.
[22] Y. Hou, C. Li and Y. Zhou, "Applications of High-Efficiency Abrasive Process with CBN Grinding Wheel", Engineering, vol. 2, no. 3, **(2010)**, pp. 184-189.
[23] F. Klocke, A. Baus and T. Beck, "Coolant induced forces in CBN high speed grinding with shoe nozzle", Annals of the CIRP, vol. 49, no. 1, **(2000)**, pp. 241-244.
[24] S. -K. Lee, M. Yuji, K. Tsunemoto and S. Katsuo, "Effects of minimizing hydrodynamic pressure in ultra-precision mirror grinding", International Journal of Machine Tools & Manufacture, vol. 44, no. 10, **(2004)**, pp. 1031–1036.
[25] C. H. Li, G. Q. Cai and S. C. Xiu, "Hydrodynamic Pressure Modeling and Verification of Contact Zone on Abrasive Jet Finishing with Grinding Wheel as Restraint", Acta Armamentarii, vol. 28, no. 2, **(2007)**, pp. 202-205.
[26] S. Wang, C. H. Li and Y. C. Ding, "Investigation into Speed and Temperature Field of Metal Drop in High-melting Metal Arc Spraying", International Journal of Control and Automation, vol. 5, no. 3, **(2012)**, pp. 237-248.
[27] B. Zhang and A. Nakajima, "Hydrodynamic Fluid Pressure in Grinding Zone During Grinding With Metal-Bonded Diamond Wheels", Journal of Tribology, vol. 122, no. 2, **(2000)**, pp. 603-608.
[28] S. Wang and C. Li, "Application and Development of High-efficiency abrasive process", International Journal of Advanced Science and Technology, vol. 47, no. 10, **(2012)**, pp. 51-64.

Authors

Z. L. Han is a graduate student at the School of Mechanical Engineering of Qingdao Technological University and has a interest in grinding and abrasive finishing, in particular CNC grinding; superabrasive grinding wheels; minimum quantity lubrication (MQL) grinding; simulation of grinding processes.

C. H. Li was awarded a PhD from the Northeastern University, China, in 2006. He is now a professor at the School of Mechanical Engineering of Qingdao Technological University. His research interests include computer applications in the study of surface finish mechanism; materials removal rate; abrasive finishing; quick-point grinding; surface roughness and integrity; CNC grinding; superabrasive grinding wheels; minimum quantity lubrication (MQL) grinding; grinding temperature field modeling; simulation of grinding processes; and high speed machining.